2014 IEEE International Conference on Robotics & Automation (ICRA)
Hong Kong Convention and Exhibition Center
May 31 - June 7, 2014. Hong Kong, China

A Passivity Based Compliance Stabilizer for Humanoid Robots

Chengxu Zhou, Zhibin Li, Juan Castano, Houman Dallali, Nikos G. Tsagarakis, and Darwin G. Caldwell

Abstract— **This paper presents a passivity based compliance stabilizer for humanoid robots. The proposed stabilizer is an admittance controller that uses the force/torque sensing in feet to actively regulate the compliance for the position controlled system. The low stiffness provided by the stabilizer permits compliant interaction with external forces, and the active damping control guarantees the passivity by dissipating the excessive energy delivered by disturbances. Both the theoretical work and simulation validations are presented. The effectiveness of the stabilizer is demonstrated by the simulations of a simplified cart-table model and the multi-body model of a humanoid under impulsive/periodic force perturbations during standing and walking in place. Simulation data show the quantitative evaluation of the stabilization effect by comparing the responses of body attitude, center of mass, center of pressure without and with the stabilizer.**

I. Introduction

The significance of stabilization control had gained limited attention in the past decades while the most efforts were made to generate stable dynamic gaits. After acquiring feasible walking patterns that allow the robot to walk in an ideally defined environment, bipeds are found to be sensitive to small un-modeled uncertainties in the environment, such as unevenness of the floor, unexpected pushes, or discrepancies between the simplified model and the real system. These uncertainties most probably produce undesired energy change on the system thus cause the disturbance on the state of the robot. If the energy injected or dissipated by disturbances can be compensated, then the state of the robot would return to its desire trajectory. This inspired us to develop a stabilizer in addition to a gait pattern generator.

In order to avoid confusion, stabilizers are classified into two categories in this paper: local stabilizer and global stabilizer. This is in agreement with the short-term and long-term absorption of disturbances proposed in [1]. It is important to delineate these two concepts since the bipeds have limited attraction region to stabilize itself due to the limited support polygon. As long as the required effort to counterbalance the disturbance can be supplied by the current foot-ground contacts, the biped does not need to change its physical contact with the environment. Therefore, any control action that leads to the negative rate change of undesired energy will stabilize the state of the robot, which is denoted as local stabilization and hereafter. However, once the disturbance becomes significantly larger, the state of the robot can no longer be stabilized due to the viable force/torque limited by the current contact polygon, thereby taking steps or using upper limbs is demanded to form new contacts. These sort of control action forms an enlarged attraction region which again embraces the disturbed states, therefore, they can be classified as global stabilization.

Most past works utilized compliance or impedance control to address the local stabilization. Hashimoto et al. used a nonlinear compliance control to modify a predefined walking patter to absorb landing impacts [2]. Kajita et al. applied body posture and foot force control to track the linear inverted pendulum model with a delay of ZMP response [3]. The Cartesian impedance control was also used to stabilize torque controlled robots in standing posture [4] [5]. Hyon et al. [4] introduced damping in joint space in order to ensure local stabilization. Our earlier work in [6] [7] stabilized the position controlled robot using active compliance control to replicate the softness. However, the method in [6] used dimensionless gains without specifying the stiffness and damping, making it difficult to interpret. And the algorithms in [7] was modeled in polar coordinate particularly for standing stabilization and was not straightforward to combine with existing walking pattern formulated in Cartesian space.

For the global stabilization, some works exploited the planning of time-based trajectories by adjusting foot placement. Morisawa et al. modified the foot trajectory using the simultaneous planning of the center of mass (COM) and the ZMP [8]. Urata et al. selected the optimal pattern from a number of on-line re-planned foot and ZMP trajectories together with the preview control for balance recovery [9]. The common ground of these work is the reliance on an additional local stabilizer that damps out a portion of excessive disturbance from step to step. Alternatively, some other researchers used event-based methods. Pratt et al. proposed the Capture Point (CP) to indicate where the robot should step for a complete stop [10]. Stephens et al. used a state machine to trigger stepping and applied the model predictive control for generating recovery motion [11]. Wight et al. validated the foot placement estimator on a planar robot taking the ground impact effect into account [12].

This paper presents an effective stabilizer for local stabilization of humanoid COMAN [13] merely in the case that the disturbance won't require the robot to take steps. A passivity based admittance control is formulated based on the cart-table model [14] to achieve active compliance. Since the active compliance is obtained through control, a range of variable stiffness can be configured in additional to the COMAN's intrinsic compliance. The proposed stabilizer is generic to be applied on both stiff and compliant robots.

The paper is organized as follows. Section II elaborates

This work is supported by the FP7 European projects AMARSi (ICT-248311) and WALK-MAN (ICT-2013-10).

Authors are with the Department of Advanced Robotics, Istituto Italiano di Tecnologia, via Morego 30, 16163 Genova, Italy.
Email: name.surname@iit.it

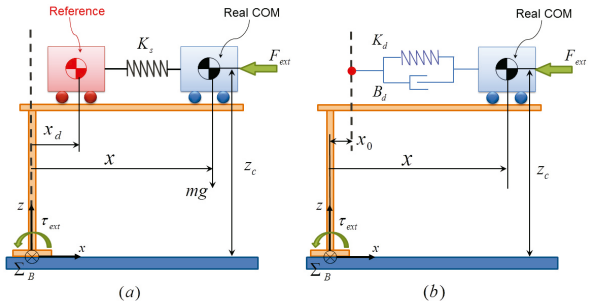

Fig. 1. Cart-table model for formulating stabilizer (sagittal view).

TABLE I

PARAMETERS FOR CONTROLLER

m:	mass of the robot
z_c:	nominal height of the COM
x_d:	desired position reference
x_s:	length of the spring deflexion
x_0:	equilibrium position
x:	real position of the COM
K_s:	resultant physical stiffness of the system
B:	real viscous coefficient of the system
K_d:	desired spring stiffness of the impedance
B_d:	desired viscous coefficient of the impedance

the control principles. Section III-A provides the simulation validation of the simplified cart-table model and proves its effectiveness. Section III-B and III-C present the implementation on the simulated multi-body model of COMAN and analyze the simulation data. The paper is concluded in Section IV.

II. CONTROL PRINCIPLES

The cart-table model introduced by Kajita et al. [14] is used to model the robot as as a simplified cart moving on a mass-less table. The table has a small support area that represents the support foot, and the cart represents the COM. Our proposed local stabilization approach is formulated based on cart-table model which can be further combined with a walking pattern generator using the same model during standing and walking. The parameters used in this paper are listed in Table I. All the equations are formulated in local frame $\sum_B$ which is located at center of the support foot.

The dynamics of the model in Fig. 1(a) is described by

$$\tau_{ext} = z_c(m\ddot{x} + B\dot{x} + K_s(x_d - x)) + \tau_g. \quad (1)$$

The term τ_{ext} is the summation of all torques generated by the external disturbances, τ_g is the torque generated by the gravity

$$\tau_g = mgx. \quad (2)$$

For the system with negligible physical damping B, the dynamics can be simplified as

$$\tau_{ext} = z_c(m\ddot{x} + K_s(x_d - x)) + \tau_g. \quad (3)$$

The cart-table model can be emulated as a spring-damper system with the gravity compensation. As shown in Fig. 1(b), a desired spring K_d ($K_d < K_s$) and a damper B_d are connected between the equilibrium and the real COM. The configurable parameters are the stiffness and damping, while the inertia property is not modulated. Hence, given the equilibrium x_0, the dynamics of this desired system is

$$\tau_{ext} = z_c(m\ddot{x} + B_d(\dot{x_0} - \dot{x}) + K_d(x_0 - x)). \quad (4)$$

Therefore, if the net ground reaction torques in both systems are equivalent as

$$\frac{\tau_g}{z_c} + K_s(x_d - x) = B_d(\dot{x_0} - \dot{x}) + K_d(x_0 - x), \quad (5)$$

thus these two systems would have the same dynamic response from the observation at the COM level.

Note that the term $K_s(x_d - x)$ implies the possibility that by controlling x_d to satisfy (5), the torque can be controlled by an active regulation via the spring deflexion.

By rearranging (5), we obtain the formula of the referential position x_d based on the real COM position x,

$$x_d = \frac{K_d}{K_s}x_0 + \frac{K_s - K_d}{K_s}x + \frac{B_d}{K_s}(\dot{x_0} - \dot{x}) - \frac{\tau_g}{z_c K_s}. \quad (6)$$

The above method modulates the position reference to achieve a desired impedance based on the feedback of COM position and velocity. The control law can be reformulated by the relation between torque and spring deflexion. Denote by τ the torque applied at the system in $\sum_B$, we have

$$\begin{cases} \tau &= -K_s x_s, \\ x &= x_d + x_s. \end{cases} \quad (7)$$

So x and $\dot{x}$ can be obtained as

$$\begin{cases} x &= x_d - \frac{\tau}{z_c K_s}, \\ \dot{x} &= \dot{x}_d - \frac{\dot{\tau}}{z_c K_s}. \end{cases} \quad (8)$$

Substitute (8) into (6), yields

$$\begin{aligned} x_d =& \frac{K_d}{K_s}x_0 + \frac{B_d}{K_s}\dot{x}_0 + \frac{K_s - K_d}{K_s}x_d - \frac{B_d}{K_s}\dot{x}_d \\ &- \frac{K_s - K_d}{z_c K_s^2}\tau + \frac{B_d}{z_c K_s^2}\dot{\tau} - \frac{\tau_g}{z_c K_s}. \end{aligned} \quad (9)$$

The desired velocity $\dot{x}_d$ can be replaced by the derivative of the x_d in a discrete form

$$\dot{x}_d = \frac{x_d(i) - x_d(i-1)}{\Delta t}, \quad (10)$$

where Δt is the sampling time.

Substitute (10) into (9), we can derive the desired reference position x_d in a discrete form at the i th control loop, given the feedback $\tau(i)$,

$$x_d(i) = \frac{\Delta t}{K_d \Delta t + B_d}A(i) + \frac{B_d}{K_d \Delta t + B_d}x_d(i-1), \quad (11)$$

where A is an intermediate variable

$$\begin{aligned} A(i) =& K_d x_0(i) + B_d \dot{x_0}(i) + \frac{K_d - K_s}{z_c K_s}\tau(i) \\ &+ \frac{B_d}{z_c K_s}\dot{\tau}(i) - \frac{\tau_g(i)}{z_c}. \end{aligned} \quad (12)$$

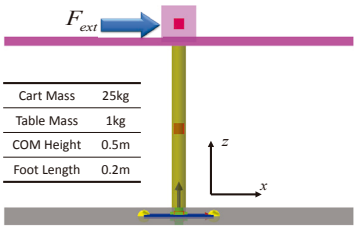

Fig. 2. Cart-Table Model used in ROBOTRAN simulation.

The gravity torque used in (12) can be approximated by

$$\tau_g(i) = mg(x_d(i-1) - \frac{\tau(i)}{z_c K_s}). \quad (13)$$

Setting $K_s \to \infty$ in (12) results in the formula for a stiff system without physical compliance, then A evolves to

$$A(i) = K_d x_0(i) + B_d \dot{x}_0(i) - \frac{\tau(i)}{z_c} - \frac{\tau_g(i)}{z_c}. \quad (14)$$

To achieve active compliant behavior as a spring-damper system, this stabilization approach uses the feedback of ground reaction torque as an input and generates the COM reference as an output. Therefore, it can be classified as an admittance controller. The force/torque is indirectly controlled by modifying the position reference, which respects the physical causality of "force→motion".

The compliance level is adjusted by the stiffness, and the passivity is warranted by applying active damping at the COM because the real damping of the system is generally insufficient. For one degree of freedom (DOF) system, (11) is the general equation to achieve the admittance control. Equation (12) is used for the system with intrinsic elasticity, whereas (14) is for a system with ideal stiff coupling between gear transmission and link. This approach can be also used for an orthogonal 2-DOF system in a decoupled form. The desired position x_d and y_d can be obtained by substituting $K_s^{x,y}$, $\tau_{x,y}$ and x_0/y_0 respectively into (11).

III. Simulations

To rigorously validate the effectiveness of the stabilizer, three simulation studies were carried out at an increasing complexity. The first simulation thoroughly analyzes the stabilizer's effect on a real cart-table system as a fundamental validation before the implementation on a multi-body model. The second one examines the standing stabilization performance on a 3D full body humanoid in a physics based simulation by Open Dynamic Engine (ODE). The third one shows a preliminary extension of walking in place stabilization.

A. Simulation Study I

As shown in Fig. 2, a 2D cart-table model is constructed using the rigid body dynamics simulator ROBOTRAN [15]. The parameters used for this simulation are as follows. The cart has $25kg$ mass with COM height z_c $0.5m$, and the table has small mass of $1kg$ with a $0.2m$ long foot. The desired stiffness and damping are $K_d = 800N/m$, $B_d = 40Ns/m$ in this simulation. The control loop runs at $1kHz$.

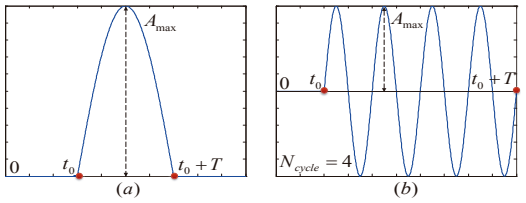

Fig. 3. (a) Impulsive and (b) Periodic disturbances.

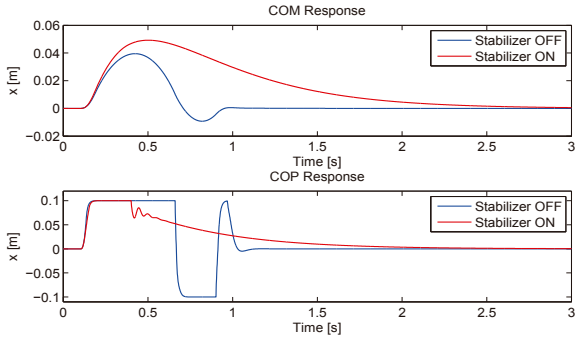

Fig. 4. COM and COP responses after impulse in ROBOTRAN simulation.

Two types of disturbances are introduced to validate the effectiveness of the proposed stabilizer: impulsive and periodic force disturbances. As shown in Fig. 3(a), an impulsive force is modeled as a half cycle sinusoid starting at t_0 with duration of T and maximum amplitude of A_{max}. The periodic force is defined as a 4-cycle sinusoid with maximum amplitude A_{max}, it is applied to the model at time t_0 and last for T which is shown in Fig. 3(b). These two disturbances allow the comparison of the system responses against disturbances without and with the stabilizer respectively.

In the first test, an impulsive force of $t_0 = 0.1s, T = 0.1s, A_{max} = 180N$ was applied to the cart in positive x direction. The amplitude of the disturbance was set in order not to completely topple the cart-table system since it cannot take a new step. The COM and COP position changes after the disturbance are shown in Fig. 4. It can be seen that the model without stabilizer acted as a rigid system, so the table tilted, resulting in the COP moved back and forth between the edges. Whereas the model with stabilizer buffered the impulsive force in a compliant manner by moving the COM along the disturbance direction, and then moved back to equilibrium. The whole system kept stable compared to the previous case, shown by the snapshots in Fig. 7.

The second test was performed by a periodic force of $t_0 = 0.1s, T = 1.5s, A_{max} = 120N$ which was applied to the cart COM in positive x direction. Fig. 5 shows the COM and COP responses after the disturbance. The stabilizer still moved forward in order to buffer the external force during the disturbance, and then eliminated the position offset as soon as the disturbance was removed. It can be also seen that in order to reject the negative disturbance, the stabilizer generate an extra torque by moving the COP to the negative direction faster than the COM.

The impacts were absorbed by the active compliance

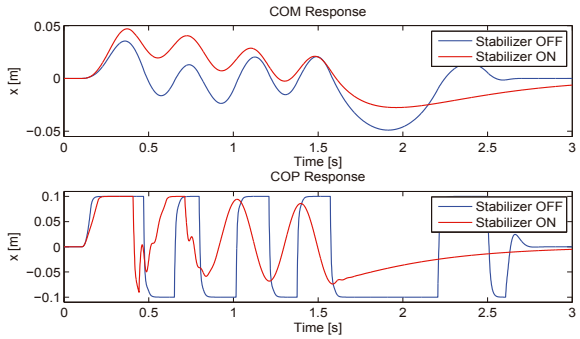

Fig. 5. COM and COP responses during periodic disturbance in ROBOTRAN simulation.

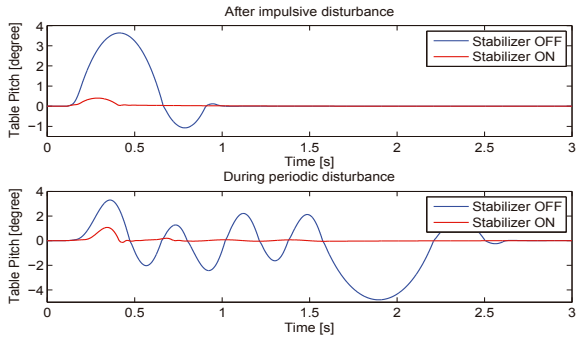

Fig. 6. Table orientation variations during (upper) impulsive and (below) periodic disturbance in ROBOTRAN simulation.

controlled by the stabilizer, so the table also kept stable orientation. The snapshots of cart-table model's responses during periodical disturbance are shown in Fig. 8. In the contrast, it is obvious that the system without stabilizer during disturbance acted as a rigid body which caused tilting and vibration of the table. The table orientation variations after impulsive and periodic disturbance are shown in Fig. 6, it shows that the stabilizer could avoid the perturbations to the system thus maintain stability compared to those without any stabilization.

B. Simulation Study II

Here, the proposed stabilizer is implemented on a multi-body humanoid robot simulated in ODE (Fig. 9) in order to test preliminary stabilization and walking control strategies prior to future implementation on the real COMAN robot. It has 6 DOFs in each leg, only these 12 DOFs are controlled during the following tests. The upper body joints are controlled at constraint position. More details of physical parameters of COMAN can be found in [13].

The desired COM equilibrium superimposed by the stabilizer's output in (11) are the inputs to the COM based inverse kinematics [7]. The joint position references solved by the inverse kinematics are sent to the on-board position controllers. The horizontal components of the resultant torque in the local feet's coordinate are computed by

$$\boldsymbol{\tau}_{x,y} = \{\boldsymbol{\tau}_l + \boldsymbol{\tau}_r + \mathbf{r}_{f_l} \times \mathbf{f}_l + \mathbf{r}_{f_r} \times \mathbf{f}_r\}_{x,y}\,, \qquad (15)$$

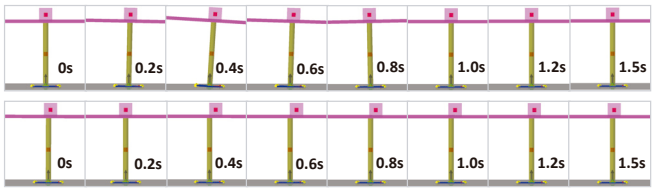

Fig. 7. Snapshots of cart-table model response during impulsive disturbance without (upper) and with (below) stabilizer in ROBOTRAN simulation.

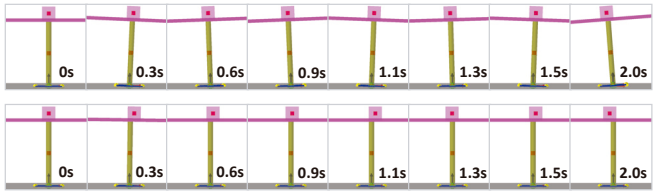

Fig. 8. Snapshots of cart-table model response during periodic disturbance without (upper) and with (below) stabilizer in ROBOTRAN simulation.

where f_l, τ_l and f_r, τ_r are the force/torque measured by the F/T sensor in each foot. r_{f_l} and r_{f_r} are the position vector from the origin of $\sum_B$ to the origin of F/T sensor in left and right foot respectively.

It should be noted that the origin of $\sum_B$ is defined as the midpoint of horizontal projections of two ankles. The global coordinates $\sum_W$ coincides with $\sum_B$ while the robot standing at the initial position. The desired stiffness and viscous coefficients used in this simulation are $K_d^x = 400N/m$, $B_d^x = 20Ns/m$ (sagittal plane), and $K_d^y = 800N/m$, $B_d^y = 100Ns/m$ (lateral plane). The equilibrium x_0, y_0 in (12) and (14) are constant here in standing posture. The control loop runs at $500Hz$.

After an initialization of $0.5s$, the center of pelvis moved to the position $(0.0023, 0, 0.4837)m$, meanwhile the calculated overall COM was at $(0.0262, 0, 0.4350)m$ which was close to pelvis center. Therefore, any disturbance applied at the pelvis were very close to the overall COM and didn't generate any distinct moment around the overall COM.

Impact tests were performed to validate the stabilization control on the full body humanoid. The results are compared with those using no stabilization control to deal with the impulsive force. Same impulsive force used in previous simulation was applied to the robot. The impulse with $T = 0.1s$, $A_{max} = 180N$ was applied to the pelvis at $t_0 = 0.6s$ along the positive direction of x, y axis respectively.

The reactions of the COM and COP after the disturbances can be seen in Fig. 10 and Fig. 11. It can be observed that robot dissipated the impulsive force by buffering the COM along the disturbed direction first, then recover to equilibrium position quickly in both tests in x, y axes after the withdrawal of disturbances. However, this reaction was not observed when the stabilizer was off.

Fig. 12 shows the joint torques of left leg after y impulse, it is found that the hip roll joint generated almost $50Nm$ for recovering balance. In contrast, no significant torque was generated while the stabilizer was off.

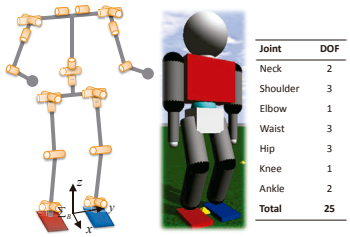

Fig. 9. Kinematics and actuator configuration of the ODE model.

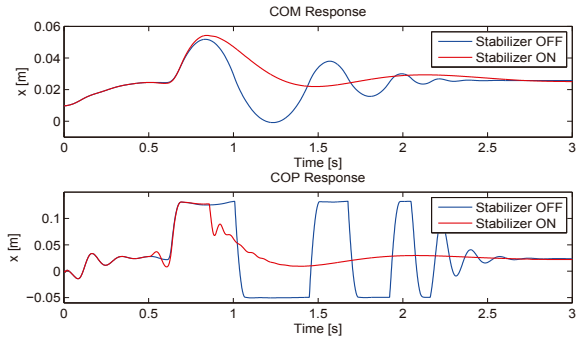

Fig. 10. COM and COP responses during x-impulsive disturbance in ODE.

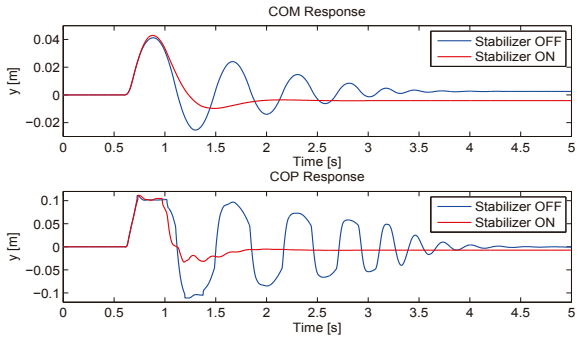

Fig. 11. COM and COP responses during y-impulsive disturbance in ODE.

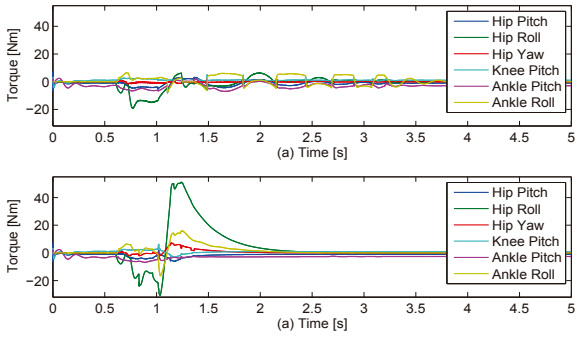

Fig. 12. Left leg joint torques (a) without (b) with stabilizer under y impulse while standing in ODE.

C. Simulation Study III

The third comparison study was carried out to evaluate to what extent the stabilizer could potentially stabilize a pre-fixed gait without any modification of the walking pattern. The effectiveness of the proposed stabilizer was validated when the simulated robot performed walking in place with a fixed walking pattern by the method in [16] [17]. The reason walking in place is chosen as a further validation is that the robot's base frame $\sum_B$ coincides with the global frame $\sum_W$ during gait. It should be noted that the proposed local stabilization is formulated in an inertial frame $\sum_B$, but this assumption would be violated during normal walking due to the displacements of support feet in x axis.

The gait starts with double support on flat ground, and the feet during walking is always level to the ground. The gait cycle is $1.0s$, the foot clearance from the ground is $0.03m$. The equilibrium y_0 in the stabilizer is substituted by the desired COM trajectory from the walking pattern in y axis. The walking starts at $0.5s$ and ends at before $8.0s$.

First, the COM responses in y direction without and with the stabilizer while walking in palace are shown in Fig. 13(a). Compared to the desired COM, it can be seen that the stabilizer improved the precision of COM tracking and tranquillized the state after walking stopped. Whereas without the stabilizer, the bigger amplitude of COM movement indicated that the robot walked more unstably and had oscillated several seconds after the last step. In general, models used for either off-line or on-line trajectory planner inevitably has discrepancy in the real robot, such that even slight modelling errors will result in unexpected behavior as time goes by. Hence, the proposed stabilizer is useful for compensating for the ground impacts caused by the mismatch between the simplified model and the real robot.

Additionally, we also evaluated the stabilizer's performance against an impulse during walking in place. To inspect more thoroughly, it is necessary to determine timing and the linear momentum applied by the impulse. The vulnerable situation during walking against impulse is at the single support phase when the COM velocity becomes 0, and the robot receives the disturbance of the direction from swing foot to the support foot. Quantitative experiments were carried out to find the maximum impulse that the robot could tolerate. The upper limits are $120N$ and $220N$ without and with the stabilizer respectively. The COM responses under the impulse of $t_0 = 1.9s, T = 0.1s, A_{max} = 180N$ are shown in Fig. 13(b). The snapshots of this test are shown in Fig. 14 spaced by 0.3 s interval. The external force was applied at the third snapshot. Without the stabilizer, robot failed to attenuate the excessive kinetic energy and eventually lost balance. In the contrast, with stabilizer though the robot tilted to left, eventually it was able to absorb a portion of additional injected energy before tipping over the support foot, and recovered walking in place after some steps.

IV. Conclusion

A stabilizer based on the principle of actively controlling compliance at the COM level is proposed using the cart-table model. The stabilizer is proved to be effective to stabilize both the simplified cart-table system and a whole body robot in a number of designed comparison studies in this paper.

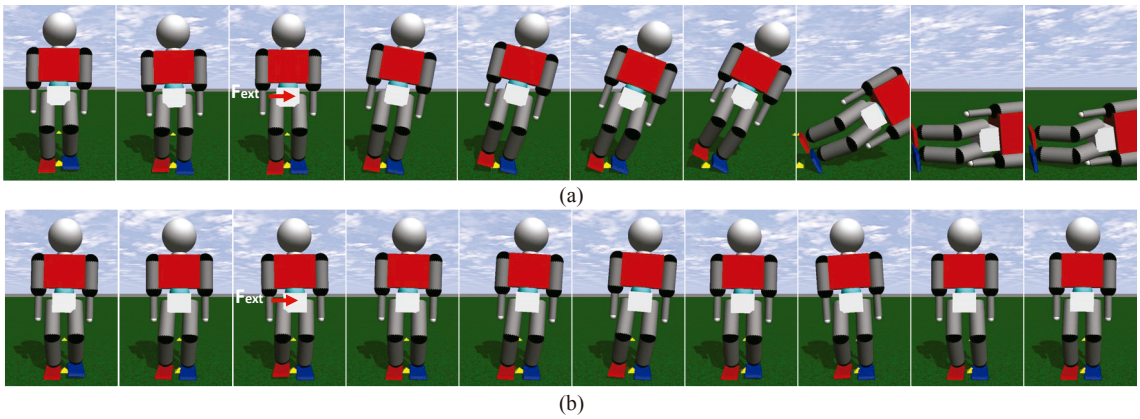

Fig. 14. Snapshots of COMAN's reaction (a) without and (b) with stabilizer under y impulse while walking in place in ODE.

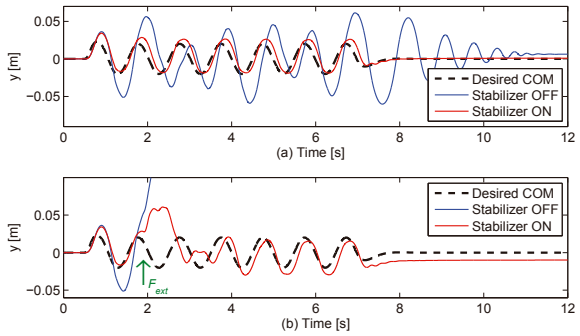

Fig. 13. COM responses in y direction (a) without disturbance (b) under y impulse while walking in place in ODE.

As a local stabilization technique, the proposed stabilizer achieves its functionality by simplicity yet robustness against various disturbances during standing and walking in place. Even for a pre-fixed walking pattern, our stabilizer could already provide prominent self-stability of walking without re-planning the gait. Therefore, the proposed stabilizer is promising to be integrated into a control architecture with gait re-planning at a higher layer in order to produce a more adaptive and robust walking. Additionally, it requires reformulation of this stabilizer by using the new support foot as the base frame alternatively during walking, which will be the main extension for the future work.

REFERENCES

[1] T. Sugihara and Y. Nakamura, "Whole-body cooperative balancing of humanoid robot using cog jacobian," in *IEEE/RSJ International Conference on Intelligent Robots and Systems*, vol. 3, 2002, pp. 2575–2580.

[2] K. Hashimoto, Y. Sugahara, H. Sunazuka, C. Tanaka, A. Ohta, M. Kawase, H. Lim, and A. Takanishi, "Biped landing pattern modification method with nonlinear compliance control," in *IEEE International Conference on Robotics and Automation*, May 2006, pp. 1213 –1218.

[3] S. Kajita, M. Morisawa, K. Miura, S. Nakaoka, K. Harada, K. Kaneko, F. Kanehiro, and K. Yokoi, "Biped walking stabilization based on linear inverted pendulum tracking," in *IEEE/RSJ International Conference on Intelligent Robots and Systems*, 2010, pp. 4489–4496.

[4] S. Hyon, J. Hale, and G. Cheng, "Full-body compliant human-humanoid interaction: Balancing in the presence of unknown external forces," *IEEE Transactions on Robotics*, vol. 23, no. 5, pp. 884–898, October 2007.

[5] C. Ott, M. Roa, and G. Hirzinger, "Posture and balance control for biped robots based on contact force optimization," in *IEEE-RAS International Conference on Humanoid Robots*, Bled, Slovenia, 2011, pp. 26–33.

[6] Z. Li, B. Vanderborght, N. G. Tsagarakis, L. Colasanto, and D. G. Caldwell, "Stabilization for the Compliant Humanoid Robot COMAN Exploiting Intrinsic and Controlled Compliance," in *IEEE International Conference on Robotics and Automation*, USA, 2012, pp. 2000–2006.

[7] Z. Li, N. Tsagarakis, and D. G. Caldwell, "A passivity based admittance control for stabilizing the compliant humanoid COMAN," in *IEEE-RAS International Conference on Humanoid Robots*, Osaka, Japan, Nov. 29th - Dec. 1st 2012, pp. 44–49.

[8] M. Morisawa, K. Harada, S. Kajita, K. Kaneko, J. Sola, E. Yoshida, N. Mansard, K. Yokoi, and J. Laumond, "Reactive stepping to prevent falling for humanoids," in *IEEE-RAS International Conference on Humanoid Robots*, Paris, France, December 7-10 2009, pp. 528–534.

[9] J. Urata, K. Nshiwaki, Y. Nakanishi, K. Okada, S. Kagami, and M. Inaba, "Online decision of foot placement using singular LQ preview regulation," in *IEEE-RAS International Conference on Humanoid Robots*, 2011, pp. 13–18.

[10] J. Pratt, J. Carff, S. Drakunov, and A. Goswami, "Capture point: A step toward humanoid push recovery," in *IEEE-RAS International Conference on Humanoid Robots*, December 2006, pp. 200–207.

[11] B. Stephens and C. Atkeson, "Push recovery by stepping for humanoid robots with force controlled joints," in *IEEE-RAS International Conference on Humanoid Robots*, 2010, pp. 52–59.

[12] D. Wight, E. Kubica, and D. Wang, "Introduction of the foot placement estimator: A dynamic measure of balance for bipedal robotics," *Journal of Computational and Nonlinear Dynamics*, vol. 3, no. 1, pp. 011 009–011 019, 2008.

[13] N. Tsagarakis, S. Morfey, G. Medrano-Cerda, Z. Li, and D. Caldwell, "Compliant humanoid coman: Optimal joint stiffness tuning for modal frequency control," in *IEEE International Conference on Robotics and Automation*, 2013, pp. 665–670.

[14] S. Kajita, F. Kanehiro, K. Kaneko, K. Fujiwara, K. Harada, K. Yokoi, and H. Hirukawa, "Biped walking pattern generation by using preview control of zero-moment point," *IEEE International Conference on Robotics and Automation*, pp. 1620–1626, 2003.

[15] H. Dallali, M. Mosadeghzad, G. A. Medrano-Cerda, N. Docquier, P. Kormushev, N. Tsagarakis, Z. Li, and D. Caldwell, "Development of a dynamic simulator for a compliant humanoid robot based on a symbolic multibody approach," in *IEEE International Conference on Mechatronics*, 2013, pp. 598–603.

[16] Z. Li, N. Tsagarakis, and D. G. Caldwell, "Walking Trajectory Generation for Humanoid Robots with Compliant Joints: Experimentation with COMAN Humanoid," in *IEEE International Conference on Robotics and Automation*, Minnesota, USA, May 2012.

[17] Z. Li, N. G. Tsagarakis, and D. G. Caldwell, "Walking pattern generation for a humanoid robot with compliant joints," *Autonomous Robots*, vol. 35, no. 1, pp. 1–14, 2013.